

We are IntechOpen, the world's leading publisher of Open Access books Built by scientists, for scientists

6,000

Open access books available

148,000

International authors and editors

185M

Downloads

Our authors are among the

154

Countries delivered to

TOP 1%

most cited scientists

12.2%

Contributors from top 500 universities



WEB OF SCIENCE™

Selection of our books indexed in the Book Citation Index
in Web of Science™ Core Collection (BKCI)

Interested in publishing with us?
Contact book.department@intechopen.com

Numbers displayed above are based on latest data collected.
For more information visit www.intechopen.com



Boron Nitride Fabrication Techniques and Physical Properties

Thamer A. Tabbakh, Prashant Tyagi, Deepak Anandan, Michael J. Sheldon and Saeed Alshihri

Abstract

The III-nitride semiconductors are known for their excellent extrinsic properties like direct bandgap, low electron affinity, and chemical and thermal stability. Among III-nitride semiconductors, boron nitride has proven to be a favorable candidate for common dimension materials in several crystalline forms due to its sp^2 - or sp^3 -hybridized atomic orbitals. Among all crystalline forms, hexagonal (h-BN) and cubic (c-BN) are considered as the most stable crystalline forms. Like carbon allotropes, the BN has been obtained in different nanostructured forms, e.g., BN nanotube, BN fullerene, and BN nanosheets. The BN nanosheets are a few atomic layers of BN in which boron and nitrogen are arranged in-planer in hexagonal form. The nanostructure sheets are used for sensors, microwave optics, dielectric gates, and ultraviolet emitters. The most effective and preferred technique to fabricate BN materials is through CVD. During the growth, BN formation occurs as a bottom-up growth mechanism in which boron and nitrogen atoms form a few layers on the substrate. This technique is suitable for high quality and large-area growth. Although a few monolayers of BN are grown for most applications, these few monolayers are hard to detect by any optical means as BN is transparent to a wide range of wavelengths. This chapter will discuss the physical properties and growth of BN materials in detail.

Keywords: boron nitride, nanosheets, CVD, PLD, h-BN

1. Introduction

The III-nitride semiconductors are known for their excellent chemical and physical properties like direct bandgap, low electron affinity, and chemical and thermal stability [1–6]. Among III-nitride materials, Boron nitride (BN) is the only binary material that shows crystal polymorphism, i.e. BN can exhibit several crystal structures. This polymorphism is due to the sp^2 - or sp^3 -hybridized atomic orbital. The number of B and N atoms in BN structures is equal. BN exists in the form of hexagonal crystalline phase (h-BN), cubic (c-BN), wurtzite (w-BN), and rhombohedral (r-BN). Among all the crystalline phases, the hexagonal and cubic are the most stable phases [7, 8]. The c-BN exhibits a zinc blende structure consisting of boron and nitrogen atoms arranged tetrahedrally, like a diamond.

In contrast, h-BN exhibits a layered structure, with neighboring B and N atoms forming honeycomb structures for each sp^2 -bonded monolayers. The layers are made up of AA' stacking configuration and bounded by weak van der Waals forces with an interlayer distance of 3.33 Å, similar to graphite structure. Because of the said reason, the h-BN is a layered material and can be easily exfoliated to even a single monolayered material. The monolayered material is also known as 2D material or low-dimensional material. The h-BN material has extraordinary properties, remarkable thermal conductivity, mechanical strength, high thermal and chemical stability, and a wide bandgap. Traditionally, the BN material is used for high-temperature applications such as furnaces insulation, furnace crucibles, metal casting molds, and high-temperature lubrication [9–13]. H-BN supplemented with extraordinary physical properties exhibits atomic smoothness and a lack of dangling bond on the surface. This material in 2D form is considered the best substrate for graphene electronics [14, 15]. Moreover, 2D h-BN sheets are being explored for their application as spacer layers for metal–insulator–metal devices and as a dielectric material for transistors and nanocapacitors [16–19].

The first growth of h-BN was reported by Paffett et al. in 1990; the group used an ultrahigh vacuum (UHV) system to deposit h-BN on Pt (111) substrates [19]. The Borazine ($B_3H_6N_3$) was used as a precursor for the growth. Various surface analysis techniques were used to characterize the grown epilayers. It was observed that h-BN monolayers were grown successfully, but thick layered h-BN growth was impossible [20]. In the year of 1995, Nagashima et al. investigated the h-BN epilayers on Ni (111), Pd (111), and Pt (111). They found that the structure of the h-BN monolayer was independent of the metal substrate [21]. Furthermore, researchers found that the BN layer formed on Ni (111) did not grow layer by layer after forming the first BN monolayer. Consequently, the non-layer-by-layer growth reduced the BN growth rate significantly due to the thermal stability of the first monolayer on the Ni (111) substrate. In addition, the bond between the BN epilayers and Ni (111) surface was weaker than graphite [22]. Later, it was discovered that h-BN forms a nanotech structure with periodic nanometer-sized holes due to the significant lattice mismatch with respect to the metal substrate [23]. In 2003, the h-BN monolayer was first observed by Auwarter et al. on Ni (111) substrates and trichloro borazine (Cl_3BNH)₃. The achieved monolayer had a very low defect density and triangular domain.

Moreover, different domains with fcc and hcp boron stacking were observed. To use low-dimensional h-BN material, researchers need to find a scalable growth method. Chemical vapor deposition (CVD) is commercially used in large-area growth techniques; researchers were able to grow centimeter-scaled h-BN epilayers on various metal substrates, e.g. Ni, Cu, and Pt [24–29]. However, researchers around the globe are still working to achieve larger-sized single crystals to study the growth mechanism and ensure its feasibility in the industry. The thickest monolayer single crystal formed to date is ~500 μm [24].

The advantage of using a transition metal as a substrate is their epitaxial relationship, which enables BN films to be easily transferred to another substrate for device fabrication or material characterization [30, 31]. However, this transfer process is unreliable as it is highly dependent on the manual handling expertise of the user transferring large-area films. Furthermore, impurities induced by the solvents during the transfer process are inevitable. Therefore, to avoid considerable degradation to the h-BN film, enhancing the transfer process or introducing a direct growth method would be advantageous. At the same time, the h-BN production cost is another factor that needs to be considered before commercialization. The most common precursors

for the growth of BN are ammonia and borane [32–38]. This compound is relatively stable in air, less toxic, and easy to handle. These precursors are the most popular due to their high yield and high-quality h-BN films, but the cost of these precursors is relatively high and unpredictable. Apart from ammonia and borane, researchers are working on other less toxic precursors, e.g. borazine, trichloro borazine, diborane, dimeric diborazane + trimeric triborazane, $\text{BF}_3 + \text{N}_2 + \text{H}_2$, and trimethylamine borane [32]. To be widely accepted in the industry for mass production, the precursors should be low in toxicity, provide high yield, and be economical in price. Therefore, exploring economical and low-toxic alternatives is still in high demand. In upcoming sections, we will explain structural properties, growth/fabrication technique, and BN (low dimension) application.

2. Structure

Attributed to atomic bonding, hexagonal boron nitride (h-BN) (graphite-like) and cubic polymorph (c-BN) (diamond-like) are critical materials for a wide range of material applications with small interface traps. Unlike SiO_2 and high-k materials, h-BN materials possess an excellent interface with high mobility on different 2D materials transistors. Interestingly, super-hard BN exhibits a polymorphs phase, such as zincblende BN, hexagonal BN, wurtzite BN (w-BN), BN fullerene, BN nanotubes, and amorphous BN, which can be regarded as counterpart systems of graphite, cubic-diamond (C-diamond), hexagonal-diamond (H-diamond), carbon nanotubes (CNTs), fullerene, and amorphous carbon [39]. Due to their excellent optical and mechanical properties, w-BN and c-BN have attracted massive attention for various applications. However, at different process techniques (pressure and temperature changes), BN always faces state changes, i.e. through cold-compressing h-BN exhibits metastable w-BN instead of stable c-BN. Wen et al. suggest there might be another intermediate state between hexagonal and wurtzite-phase BN and proposed a new BN-phase (bct-BN) with considerable stability and excellent mechanical properties. The resulting bonding changes their electrical and mechanical properties through the process steps, such as superconductivity and hardness [39].

2.1 Hexagonal boron nitride (h-BN)

Hexagonal BN (h-BN) structure is similar to graphite. The h-BN consists of sp^2 -hybridized alternating B and N atoms, which are held together by a covalent bond in a hexagon (honeycomb) lattice structure, as shown in **Figure 1**. For a fully ordered crystal structure, the lattice constant of the boron nitride structure has lattice parameters: $a = 2.504\text{\AA}$ and $c = 6.661\text{\AA}$ [41]. The h-BN has six-membered rings, with boron atoms in one layer as the nearest neighbors to the N atoms in adjacent layers [40].

2.2 Cubic boron nitride (c-BN): Diamond-like

Cubic-phase BN has significant technological applications. The c-BN is the second hardest material, which is resistant to oxidation. It has a natural protective coating and is sought for its protective properties for infrared and visible spectrum applications. Cubic c-BN is also compatible with high-temperature and high-power applications; unlike diamond, c-BN can be doped with p and n type to make a high-power photodiode. The c-BN possesses a zincblende structure with ABCABC... stacking

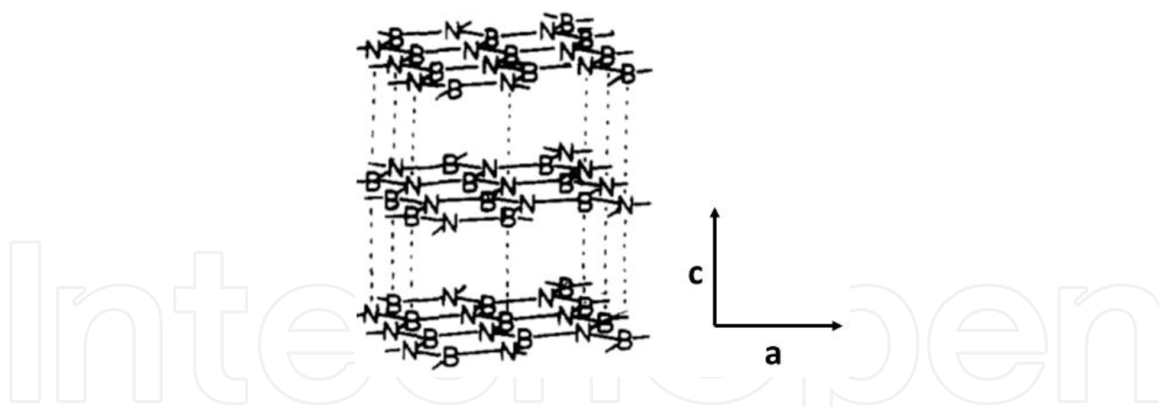


Figure 1.
Schematic diagram of the atomic configuration of layered h-BN [40].

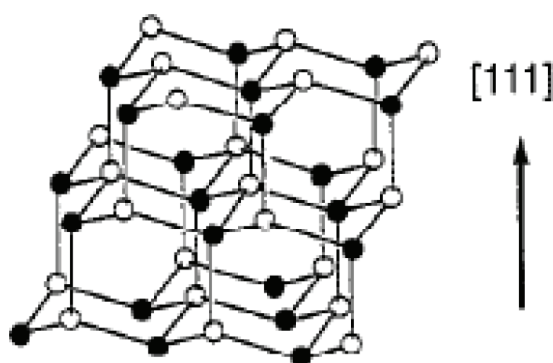


Figure 2.
Diamond structure for c-BN (lattice constant $a = 3.6153\text{\AA}$) [42].

sequence arrangements, consisting of tetrahedrally coordinated boron and nitrogen atoms with $\{111\}$ plans. The atomic arrangement of B and N atoms in the c-BN lattice is represented in **Figure 2** by the ball and stick model.

2.3 Wurtzite boron nitride

Metastable-phase stacking sequence produces additional sp^3 - and sp^2 -bonded phase forms in polytype crystal structures. For example, the stacking relationship between wurtzite (w-BN) and sp^3 -bonded cubic phases of boron nitride is analogous to that between cubic and h-BN. W-BN consists of two layers (0002 planes) structurally identical to the (111) plan c-BN. These ABC stacking arrangements yield additional metastable rhombohedral boron nitride (r-BN) crystal phase [42]. The atomic planer arrangement in w-BN and r-BN is shown in **Figure 3**.

2.4 Octahedral model: BN fullerenes

Ultrathin layer BN (typically $<3\text{ nm}$) forms fullerenes under in situ electron irradiation. The BN fullerenes exhibit B/N stoichiometry of ~ 1 . Also, fullerenes revealed unusual polyhedral electron microscope images based on microscope projection, i.e. *Nested* BN fullerenes and *single cell* fullerenes square-like and rectangle-like outlines, respectively [43]. The structure of BN fullerene is shown in **Figure 4** with the help of the ball and stick model. In **Figure 4**, the black ball represents B and the white ball represents N.

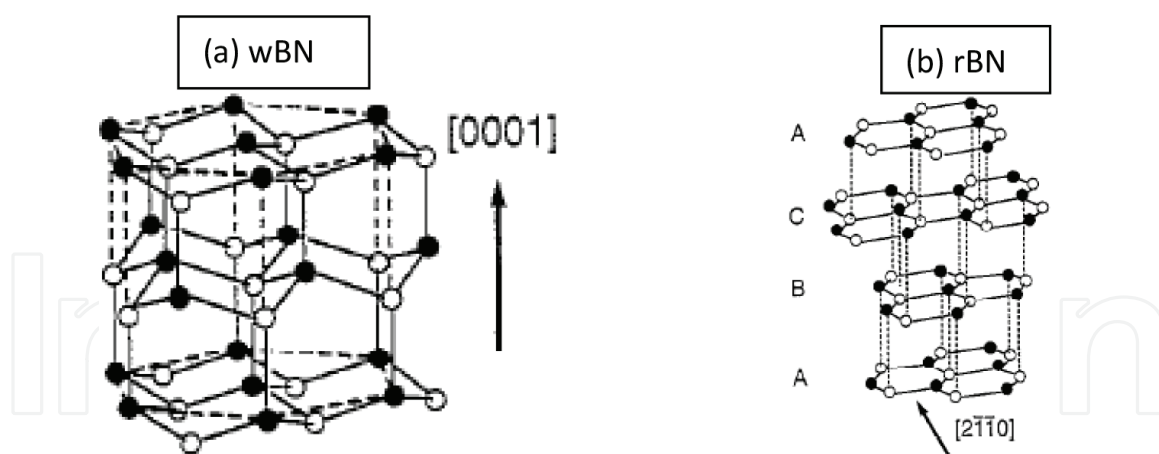


Figure 3.
 (a) Sp^3 -bonded-phase wBN (lattice constant $a = 2.5505\text{\AA}$ and $c = 4.210\text{\AA}$) (b) Sp^2 -bonded-phase rBN (lattice constant $a = 2.5042\text{\AA}$ and $c = 9.99\text{\AA}$) [42].

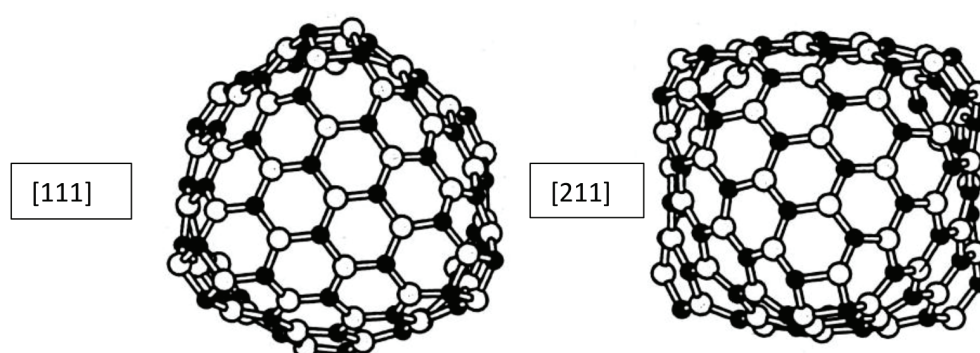


Figure 4.
 $3D$ octahedral B_7N_7 molecule in $[111]$ and $[211]$ orientation [43].

2.5 Amorphous BN

BN exhibits amorphous nature when it reacts with cesium metal. After heat treatment, the amorphous nature is transformed into turbostratic nature (tubular and corpuscles morphology) with a diameter of $3\ \mu\text{m}$ for 50 to $100\ \mu\text{m}$. The researchers observed that the interlayer distance was 3.5\AA [44].

3. Defects

As we know, BN is a good choice for low-dimensional semiconductors (especially 2D) with remarkable thermal, mechanical, and dielectric properties. Theoretically, BN should exhibit perfect lattice structures free from defects, but as we know, the actual material is marginally different from theoretical models. Similarly, BN has some inevitable structural defects that arise due to the imperfection of the growth/preparation processes. These defects are unintentionally induced because of the dramatic influence over the material's physical properties, even in a low-dimensional state.

3.1 Point defect

The point defect, known as Stone-Wales (SW), is prevalent in semiconductor materials. It involves the connectivity change of π -bonded carbon atoms leading to

their rotation by 90° [45]. This defect forms two separate vertically bonded rings instead of two rings sharing a common edge. This specific structural defect, such as graphene, is common in sp^2 -bonded carbon allotropes. Similarly, SW or point defects are observed in BN material with low dimensions [46]. The formation of point defects in BN nanoribbons is due to the structural geometry. The SW defects in BN nanoribbons (zigzag and armchair) are shown in **Figure 5**. These defects decrease the bandgap regardless of BN nanoribbon orientation but maintain ultrawide bandgap behavior (insulating). At the same time, the defect site of this particular nature is far more reactive when compared to the defect-free site in BN nanoribbon [47–49].

Atomic vacancy is also a point defect observed by high-resolution transmission electron microscopy (HRTEM). The HRTEM analysis of BN monolayers reveals triangle-shaped vacancies that have been observed. It is also revealed that the monovacancy of boron (V_B) and the monovacancy of nitrogen (V_N) coexist in nature. The boron atom has low knock-on energy compared to that of nitrogen. Hence, it favors the formation of boron vacancies rather than nitrogen vacancies [49]. Therefore, V_N is not observed during HRTEM observation.

On the other hand, the coexisting vacancies like V_B , V_{3B+N} , and V_{6B+3N} , etc., are evident. However, Alem et al. suggested that besides knock-on damage, there might be other mechanisms of forming coexisting vacancies, such as replacing ejected atoms with nearby atoms [50]. Furthermore, the interlayer distance with a missing boron atom was enlarged, which indicates that the dangling bonds for each N atom might be repulsive to each other. No stable divacancy (V_{BN}) was observed as V_{BN} would immediately transform into V_{3B+N} due to further removal of boron atoms [48].

3.2 Defect lines

Another defect observed in BN 2D material is *defect lines*, which form due to the difference in polarities of h-BN. This difference in polarity results in the convergence of N-terminated edges from domains with 60° rotation differences. These defects are observed when h-BN epilayers grow on lattice-matched substrates like Cu (111) or Ni (111). However, in situ observation of such defect lines is not detected yet. Therefore, determining adatom species migration during this defect needs further detailed study [51].

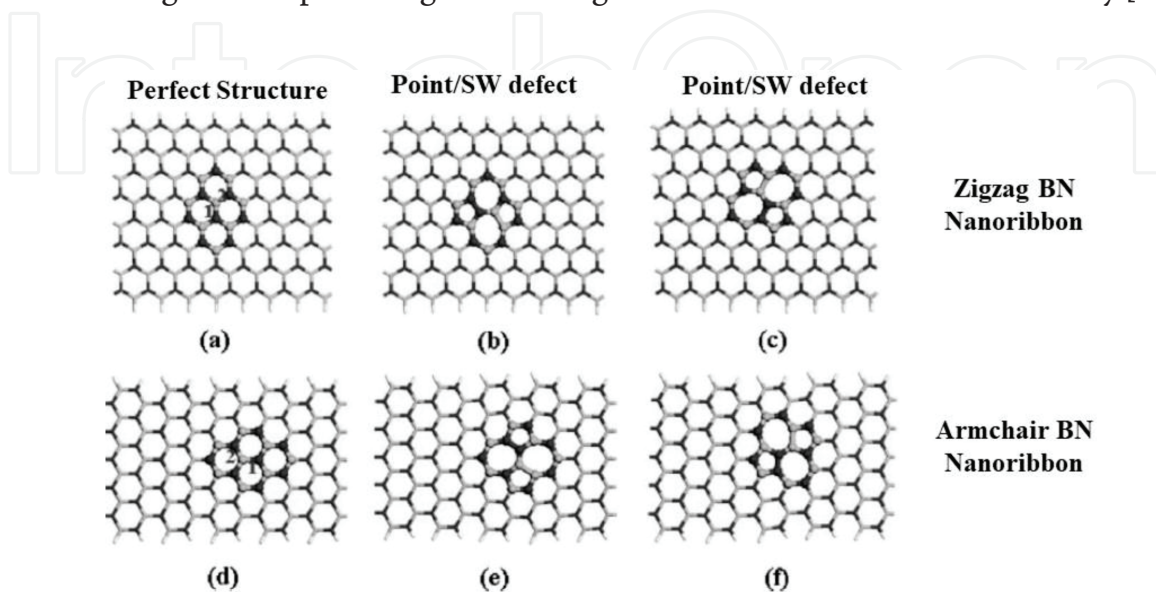


Figure 5. Two types of B-N bonds are zigzag BN nanoribbon and armchair BN nanoribbon with their defects [46].

3.3 Adlayer defect

The *adlayer defect* is another major defect observed in low-dimensional 2D h-BN. During growth, after a few layers on the metal substrate, Cu islands form structures that are observed along the grain boundaries of h-BN films. Close observation shows that grain boundaries facilitate this island's growth. From the scanning electron microscopy observation, it was found that angular islands with truncated edges were observed. The edges resemble pyramids [51]. Some other 2D materials like MoS₂ and WS₂ were observed [52, 53]. A similar observation was found during the growth of III-V nanostructures on metal substrates. It was revealed by an X-ray photoelectron spectroscopy (XPS) study that a metal grain boundary acts as the favorable energy site for the nucleation of III-V pyramid islands. Correspondingly, during the growth of h-BN monolayers, it was observed that the orientation of adlayers is strongly affected by the crystalline substrate facets [54–56].

4. Preparation methods

4.1 Mechanical exfoliation

Mechanical exfoliation has been considered the simplest way to prepare high-quality 2D material. The mechanical exfoliation employs exterior force to overcome weak van der Waals interactions between material layers. The most frequently used method is scotch tape removal. In this method, the pulling action breaks down the weak van der Waals interactions between the layers. Pacile et al. used the same method to isolate BN nanosheets from the powdered h-BN pellet (hard-pressed). By repeating the peeling and pressing process, monolayered BN nanosheets were obtained. They have reported a strong relationship between h-BN nanosheet defects and captured excitons' recombination intensity [57]. Therefore, this technique is suitable for small-scale sample preparations, only for the laboratories, which is the main drawback of this technique. Another mechanical exfoliation method that uses shear force is ball milling. This method introduces fewer point defects compared to other mechanical methods. At the same time, this method is more efficient than the scotch tape method. According to Li et al., the controlled ball milling parameters are the key to producing relatively large in-plane BN nanosheets samples. They used h-BN powder with a benzyl benzoate (C₁₂H₁₂O₂) milling agent and successfully achieved 0.3–1 μm diameter flakes with thickness between 20 and 110 nm [58].

4.2 Thermal exfoliation

For the fundamental studies, mechanical exfoliation can produce small samples of a single h-BN sheet. However, the thermal exfoliation route is more convenient if some large production is needed, such as micro- or nanofillers in polymer composites. Therefore, Cui et al. attempted a large-scale thermal exfoliation of h-BN using the easy and scalable thermal oxidation approach [59]. They observed that heating h-BN in the presence of air adds oxygen to the lattice. After heating, the material was stirred in deionized water for several minutes resulting in a thick mixture that exfoliates to form hydroxylated boron nitride without the need for sonication (or mild sonication required to increase the yield). Furthermore, Yu et al. prepared the hydroxylated boron nitride by heating h-BN powder to 1000°C inside the tubular furnace. This

process yields a similar material as Cui et al.; the prepared material was collected, mixed with binders, and stirred to obtain flakes of h-BN [60].

4.3 Chemical vapor deposition

Chemical vapor deposition (CVD) is widely used to grow various materials. **Figure 6** shows the schematic diagram of the basic CVD growth technique. CVD is the industrialized large-area growth process, which uses liquid precursors and process gases to grow the material on the desired surface at elevated temperatures. In earlier studies, researchers used diborane and ammonia as precursors for the deposition of h-BN nanosheets on various metal substrates [61]. CVD growth of BN nanosheets is the primary approach to achieving large-area growth. The large-area growth involves suppressing the nucleation sites and enhancing the 2D growth mode. The nucleation could further be suppressed using atomically flat surfaces and optimized CVD parameters [32, 62].

Additionally, using a metal substrate can enhance the surface migration, further enhancing the domains' size by suppressing nucleation and growth rate due to solid gas reactions involving the metal surface chemistry [63]. The type of precursors could be a separate boron or nitrogen source, e.g. for boron source BF_3 and NH_3 , BCl_3 and NH_3 , and B_6H_6 and NH_3). Otherwise, it could also be a single precursor like ammonium borane and borazine [64–66]. **Table 1** lists some conventional and advanced precursors in the trend to grow BN through the CVD technique. **Figure 6** illustrates the basic schematic of the horizontal CVD apparatus [76]. The apparatus consists of a horizontal quartz tube with three heater zones that provide even temperature gradient control throughout the reacting zone (inside the tube). From one side, gaseous precursors are introduced, which take part in the growth zone and precipitate (or epitaxially deposited) onto the surface of the substrate. The epitaxial growth mechanism is governed by the boundary layer adsorption phenomenon. For growth,

Precursors	Results	Reference
Ammonia borane	Single crystalline, domain size in centimeter, monolayers, and multilayers were fabricated.	[34, 36, 38, 67]
Trimethylamine borane	h-BN monolayers successfully grown on copper using organic precursor carbon doping could be achieved.	[68]
Trimethylborate, O_2 , and NH_3	h-BN monolayers were successfully grown on Rh/YSZ/Si (111) multilayer substrate, an economical and less toxic process.	[69]
Borazine (HBNH_3)	Growth of monolayer BN nanosheets having domain size in mm.	[70, 71]
Diborane and NH_3	BN nanosheets for up to 100 layers were achieved. Crystalline quality depends on the substrate, growth time, and rate.	[72, 73]
BCl_3 , NH_3 , N_2 , and H_2	h-BN nanosheets were vertically aligned on the substrate. The thickness of the aligned nanosheets is less than 10 nm.	[74, 75]

Table 1. List of conventional precursors used in CVD method for BN nanosheets/nanostructure growth.

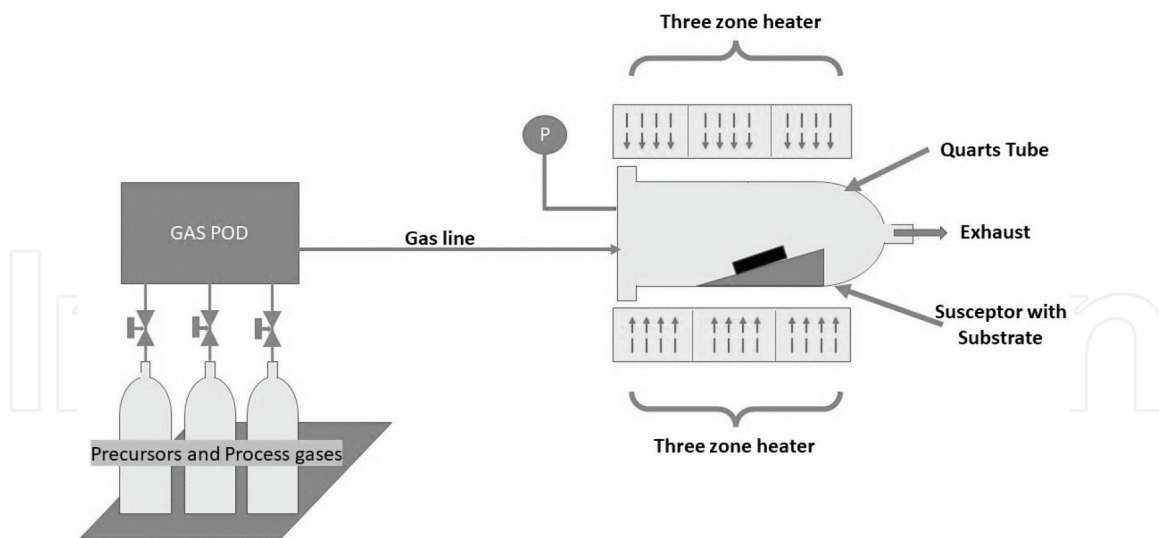


Figure 6.
Schematic diagram of basic CVD growth apparatus.

the substrate is placed over an inclined susceptor generally made up of graphite, and the inclined angle may vary from 7° to 15° . This inclination provides uniform gas flow over the susceptor and suppresses the parasitic gas-phase reactions [76, 77].

4.4 Pulsed laser deposition

Pulsed laser deposition (PLD) is a novel growth technique for the growth of III-V semiconductors. PLD is an ultrahigh vacuum technique with the base pressure ranging from $\sim 10^{-7}$ to 10^{-9} torr. As the growth takes place in a high vacuum, there is a slim chance of impurity incorporation due to contamination. In this technique, the pure material is ablated with the help of a high-energy laser at the same time the process

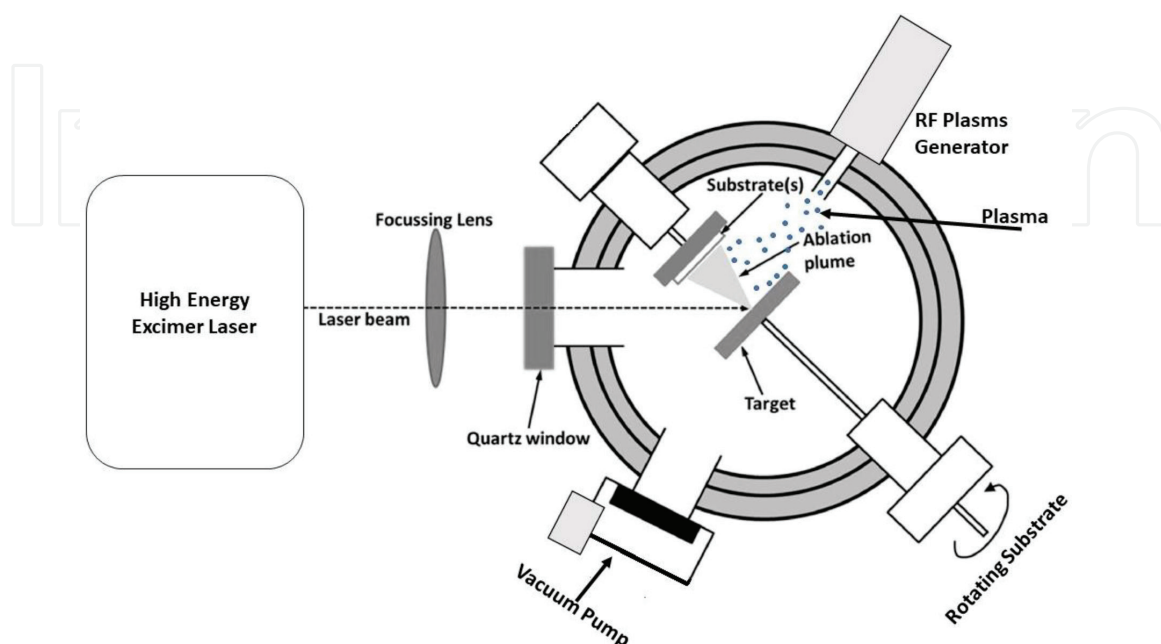


Figure 7.
Schematic diagram of PLD technique [70].

gas plasma is introduced into the chamber. The laser-ablated material reacts with plasma species and migrates on the substrate surface [55]. Recently, this technique has been used to grow h-BN nanosheets and nanostructures. **Figure 7** shows the schematic diagram of the PLD technique for reference [78]. Glavin et al. reported this method's direct growth of BN nanosheets on the sapphire substrate. The growth was carried out using BN sintered target, which took place at 700°C growth temperature. The grown film exhibits a narrow Raman line width of $\sim 30 \text{ cm}^{-1}$, providing excellent crystalline quality. Later, the prepared films were probed for their UV response, and BN thin films show deep UV detection capabilities [79]. Velázquez et al. directly grown few monolayers of h-BN on Ag/SrTiO₃(001). It was found that the grown h-BN monolayers were in the sub-millimeter range and scattered on the surface [80]. PLD is the immature technique for the growth of III-V semiconductors and is limited to small area fabrication. Very few reports on the growth of BN by the PLD technique are available. There is an immense need to study this technique to grow large-area films which could be of commercial use. There are several other methods to prepare 2D BN, like solvent exfoliation, solid state reactions, and substitution method, but only few potential large-scale preparation methods are described in this section.

5. Current application

The BN material shows excellent chemical, thermal, and mechanical properties, which are utilized in different applications. The industrial application of 2D BN is yet to be realized due to the lack of large-area thin film synthesis techniques. To date, large-area films with uniform thickness are hard to fabricate. The h-BN is known for its wide direct bandgap ($\sim 5.9 \text{ eV}$), small lattice mismatch with graphene (1.7%), and high thermal conductivity. The BN nanosheets have been employed in several semiconductors device applications, such as transparent membranes, encapsulation materials, tunneling barriers, and high dielectric materials [81]. For instance, some graphene devices fabricated on the h-BN show very high mobility in order of $60,000 \text{ cm}^2 \text{V}^{-1} \text{ s}^{-1}$, which is far greater than III-V devices that exploit 2DEG (two-dimensional electron gas) properties [82].

Interestingly, an ultrathin layer of BN is sandwiched between the graphene layer (C-BN-C), making a field effect tunneling transistor heterostructure. The study revealed that the h-BN nanosheet forms a good tunnel barrier [83]. Ranjan et al. studied dielectric breakdown failure of thin h-BN films. The study found that the breakdown field is 21 MV cm^{-1} for 3-nm-thick h-BN. The breakdown field suggests that h-BN is more suitable for gate dielectric than high-quality silicon dioxide [84].

6. Conclusion

The BN is expected to play a vital role in developing novel technologies in the future. Future technologies might include nanophotonics, nanoelectronics, quantum information, and microelectromechanical systems (MEMS) technology. Recently, researchers have been in pursuit of developing a way for large-area BN growth. As we have seen in an earlier section of this chapter, many researchers have achieved relatively large-area and high-quality growth. The large area of 2D BN material could be used to develop templates or substrates for epitaxy. It would be easier to remove from these substrates, so they could be used again for the epitaxy. By closely monitoring

the demands of semiconductor technology, it is evident that the quest for 2D large-area growth is being pursued. Therefore, further research and studies are needed to explore 2D BN limitations to understand the potential scope for new applications.

IntechOpen

Author details


Thamer A. Tabbakh¹, Prashant Tyagi², Deepak Anandan², Michael J. Sheldon² and Saeed Alshihri^{1*}

1 Director of the National Center for Nanotechnology and Semiconductors, King Abdulaziz City for Science and Technology (KACST), Material Research Science Institute, Riyadh, Saudi Arabia

2 Skyline Semiconductors Services, King Abdulaziz City for Science and Technology (KACST), Riyadh, Saudi Arabia

*Address all correspondence to: alshihri@kacst.edu.sa

IntechOpen

© 2022 The Author(s). Licensee IntechOpen. This chapter is distributed under the terms of the Creative Commons Attribution License (<http://creativecommons.org/licenses/by/3.0>), which permits unrestricted use, distribution, and reproduction in any medium, provided the original work is properly cited. 

References

- [1] Huang J-J, Kuo H-C, Shen S-C, editors. Nitride Semiconductor Light-Emitting Diodes (LEDs): Materials, Technologies, and Applications. Oxford: Woodhead Publishing; 2014
- [2] He XG et al. GaN high electron mobility transistors with AlInN back barriers. *Journal of Alloys and Compounds*. 2016;**662**:16-19. DOI: 10.1016/j.jallcom.2015.12.031
- [3] Jain SC, Willander M, Narayan J, Overstraeten RV. III-nitrides: Growth, characterization, and properties. *Journal of Applied Physics*. 2000;**87**(3):965-1006. DOI: 10.1063/1.371971
- [4] Grabowski SP et al. Electron affinity of Al_xGa_{1-x}N(0001) surfaces. *Applied Physics Letters*. 2001;**78**(17):2503-2505. DOI: 10.1063/1.1367275
- [5] Wu CI, Kahn A. Negative electron affinity and electron emission at cesiated GaN and AlN surfaces. *Applied Surface Science*. 2000;**162-163**:250-255. DOI: 10.1016/S0169-4332(00)00200-2
- [6] Moran E, editor. Boron Nitride: Properties, Synthesis, and Applications. Hauppauge, New York: Nova Science Publishers Inc.; 2017
- [7] Solozhenko VL, Turkevich VZ, Holzapfel WB. Refined phase diagram of boron nitride. *The Journal of Physical Chemistry. B*. 1999;**103**(15):2903-2905. DOI: 10.1021/jp984682c
- [8] Sokołowska A, Wronikowski M. The phase diagram (p, T, E) of boron nitride. *Journal of Crystal Growth*. 1986;**76**(2):511-513. DOI: 10.1016/0022-0248(86)90401-X
- [9] Liu L, Feng YP, Shen ZX. Structural and electronic properties of h-BN. *Physical Review B*. 2003;**68**(10):104102. DOI: 10.1103/PhysRevB.68.104102
- [10] Eichler J, Lesniak C. Boron nitride (BN) and BN composites for high-temperature applications. *Journal of the European Ceramic Society*. 2008;**28**(5):1105-1109. DOI: 10.1016/j.jeurceramsoc.2007.09.005
- [11] Jo I et al. Thermal conductivity and phonon transport in suspended few-layer hexagonal boron nitride. *Nano Letters*. 2013;**13**(2):550-554. DOI: 10.1021/nl304060g
- [12] Li C, Bando Y, Zhi C, Huang Y, Golberg D. Thickness-dependent bending modulus of hexagonal boron nitride nanosheets. *Nanotechnology*. 2009;**20**(38):385707. DOI: 10.1088/0957-4484/20/38/385707
- [13] Ouyang T, Chen Y, Xie Y, Yang K, Bao Z, Zhong J. Thermal transport in hexagonal boron nitride nanoribbons. *Nanotechnology*. 2010;**21**(24):245701. DOI: 10.1088/0957-4484/21/24/245701
- [14] Järvinen P et al. Molecular self-assembly on graphene on SiO₂ and h-BN substrates. *Nano Letters*. 2013;**13**(7):3199-3204. DOI: 10.1021/nl401265f
- [15] Garcia JM et al. Graphene growth on h-BN by molecular beam epitaxy. *Solid State Communications*. 2012;**152**(12):975-978. DOI: 10.1016/j.ssc.2012.04.005
- [16] Barati F et al. Tuning supercurrent in Josephson field-effect transistors using h-BN dielectric. *Nano Letters*. 2021;**21**(5):1915-1920. DOI: 10.1021/acs.nanolett.0c03183
- [17] Cui Z et al. Study of direct tunneling and dielectric breakdown in molecular

- beam epitaxial hexagonal boron nitride monolayers using metal–insulator–metal devices. *ACS Applied Electronic Materials*. 2020;**2**(3):747-755. DOI: 10.1021/acsaelm.9b00816
- [18] Monajjemi M. Metal-doped graphene layers composed with boron nitride–graphene as an insulator: A nano-capacitor. *Journal of Molecular Modeling*. 2014;**20**(11):2507. DOI: 10.1007/s00894-014-2507-y
- [19] Shi G et al. Boron nitride–graphene Nanocapacitor and the origins of anomalous size-dependent increase of capacitance. *Nano Letters*. 2014;**14**(4):1739-1744. DOI: 10.1021/nl4037824
- [20] Paffett MT, Simonson RJ, Papin P, Paine RT. Borazine adsorption and decomposition at Pt(111) and Ru(001) surfaces. *Surface Science*. 1990;**232**(3):286-296. DOI: 10.1016/0039-6028(90)90121-N
- [21] Nagashima A, Tejima N, Gamou Y, Kawai T, Oshima C. Electronic structure of monolayer hexagonal boron nitride Physisorbed on metal surfaces. *Physical Review Letters*. 1995;**75**(21):3918-3921. DOI: 10.1103/PhysRevLett.75.3918
- [22] Nagashima A, Tejima N, Gamou Y, Kawai T, Oshima C. Electronic dispersion relations of monolayer hexagonal boron nitride formed on the Ni(111) surface. *Physical Review B*. 1995;**51**(7):4606-4613. DOI: 10.1103/PhysRevB.51.4606
- [23] Corso M, Auwärter W, Muntwiler M, Tamai A, Greber T, Osterwalder J. Boron nitride Nanomesh. *Science*. 2004;**303**(5655):217-220. DOI: 10.1126/science.1091979
- [24] Qian Y, Kang DJ. Large-area high-quality AB-stacked bilayer graphene on h-BN/Pt foil by chemical vapor deposition. *ACS Applied Materials & Interfaces*. 2018;**10**(34):29069-29075. DOI: 10.1021/acsaami.8b06862
- [25] Zhao R, Li F, Liu Z, Liu Z, Ding F. The transition metal surface passivated edges of hexagonal boron nitride (h-BN) and the mechanism of h-BN's chemical vapor deposition (CVD) growth. *Physical Chemistry Chemical Physics*. 2015;**17**(43):29327-29334. DOI: 10.1039/C5CP04833H
- [26] Cho H et al. Growth kinetics of white graphene (h-BN) on a planarized Ni foil surface. *Scientific Reports*. 2015;**5**(1):11985. DOI: 10.1038/srep11985
- [27] Shi Y et al. Synthesis of few-layer hexagonal boron nitride thin film by chemical vapor deposition. *Nano Letters*. 2010;**10**(10):4134-4139. DOI: 10.1021/nl1023707
- [28] Preobrajenski AB, Vinogradov AS, Mårtensson N. Monolayer of h-BN chemisorbed on Cu(111) and Ni(111): The role of the transition metal 3d states. *Surface Science*. 2005;**582**(1-3):21-30. DOI: 10.1016/j.susc.2005.02.047
- [29] Li L et al. A minireview on chemical vapor deposition growth of wafer-scale monolayer h-BN single crystals. *Nanoscale*. 2021;**13**(41):17310-17317. DOI: 10.1039/D1NR04034K
- [30] Reina A et al. Large area, few-layer graphene films on arbitrary substrates by chemical vapor deposition. *Nano Letters*. 2009;**9**(1):30-35. DOI: 10.1021/nl801827v
- [31] Cartamil-Bueno SJ, Cavalieri M, Wang R, Houri S, Hofmann S, van der Zant HSJ. Mechanical characterization and cleaning of CVD single-layer h-BN resonators. *NPJ 2D Materials and Applications*. 2017;**1**(1):16. DOI: 10.1038/s41699-017-0020-8

- [32] Khan MH et al. Few-atomic-layered hexagonal boron nitride: CVD growth, characterization, and applications. *Materials Today*. 2017;**20**(10):611-628. DOI: 10.1016/j.mattod.2017.04.027
- [33] Gao Y et al. Repeated and controlled growth of monolayer, bilayer and few-layer hexagonal boron nitride on Pt foils. *ACS Nano*. 2013;**7**(6):5199-5206. DOI: 10.1021/nn4009356
- [34] Stehle Y et al. Synthesis of hexagonal boron nitride monolayer: Control of nucleation and crystal morphology. *Chemistry of Materials*. 2015;**27**(23):8041-8047. DOI: 10.1021/acs.chemmater.5b03607
- [35] Song L et al. Large scale growth and characterization of atomic hexagonal boron nitride layers. *Nano Letters*. 2010;**10**(8):3209-3215. DOI: 10.1021/nl1022139
- [36] Tay RY et al. Growth of large single-crystalline two-dimensional boron nitride hexagons on Electropolished copper. *Nano Letters*. 2014;**14**(2):839-846. DOI: 10.1021/nl404207f
- [37] Wang L, Wu B, Chen J, Liu H, Hu P, Liu Y. Monolayer hexagonal boron nitride films with large domain size and clean Interface for enhancing the mobility of graphene-based field-effect transistors. *Advanced Materials*. 2014;**26**(10):1559-1564. DOI: 10.1002/adma.201304937
- [38] Lee KH et al. Large-scale synthesis of high-quality hexagonal boron nitride Nanosheets for large-area graphene electronics. *Nano Letters*. 2012;**12**(2):714-718. DOI: 10.1021/nl203635v
- [39] Meng Y et al. The formation of sp³ bonding in compressed BN. *Nature Materials*. 2004;**3**(2):111-114. DOI: 10.1038/nmat1060
- [40] Paine RT, Narula CK. Synthetic routes to boron nitride. *Chemical Reviews*. 1990;**90**(1):73-91. DOI: 10.1021/cr00099a004
- [41] Xu B, Lv M, Fan X, Zhang W, Xu Y, Zhai T. Lattice parameters of hexagonal and cubic boron nitrides at high temperature and high pressure. *Integrated Ferroelectrics*. 2015;**162**(1):85-93. DOI: 10.1080/10584587.2015.1039410
- [42] Mirkarimi PB, McCarty KF, Medlin DL. Review of advances in cubic boron nitride film synthesis. *Materials Science & Engineering R: Reports*. 1997;**21**(2):47-100. DOI: 10.1016/S0927-796X(97)00009-0
- [43] Golberg D, Bando Y, Stéphan O, Kurashima K. Octahedral boron nitride fullerenes formed by electron beam irradiation. *Applied Physics Letters*. 1998;**73**(17):2441-2443. DOI: 10.1063/1.122475
- [44] Hamilton EJM, Dolan SE, Mann CM, Colijn HO, McDonald CA, Shore SG. Preparation of amorphous boron nitride and its conversion to a Turbostratic, tubular form. *Science*. 1993;**260**(5108):659-661. DOI: 10.1126/science.260.5108.659
- [45] Li Y, Zhou Z, Golberg D, Bando Y, von Schleyer PR, Chen Z. Stone-Wales defects in single-walled boron nitride nanotubes: Formation energies, electronic structures, and reactivity. *Journal of Physical Chemistry C*. 2008;**112**(5):1365-1370. DOI: 10.1021/jp077115a
- [46] Chen W, Li Y, Yu G, Zhou Z, Chen Z. Electronic structure and reactivity of boron nitride nanoribbons with stone-Wales defects. *Journal of Chemical Theory and Computation*. 2009;**5**(11):3088-3095. DOI: 10.1021/ct900388x

- [47] Pham T et al. Formation and dynamics of electron-irradiation-induced defects in hexagonal boron nitride at elevated temperatures. *Nano Letters*. 2016;**16**(11):7142-7147. DOI: 10.1021/acs.nanolett.6b03442
- [48] Jin C, Lin F, Suenaga K, Iijima S. Fabrication of a freestanding boron nitride single layer and its defect assignments. *Physical Review Letters*. 2009;**102**(19):195505. DOI: 10.1103/PhysRevLett.102.195505
- [49] Zobelli A, Gloter A, Ewels CP, Seifert G, Colliex C. Electron knock-on cross section of carbon and boron nitride nanotubes. *Physical Review B*. 2007;**75**(24):75-77. DOI: 10.1103/PhysRevB.75.245402
- [50] Alem N, Erni R, Kisielowski C, Rossell MD, Gannett W, Zettl A. Atomically thin hexagonal boron nitride probed by ultrahigh-resolution transmission electron microscopy. *Physical Review B*. 2009;**80**(15):155425. DOI: 10.1103/PhysRevB.80.155425
- [51] Tay RY. *Chemical Vapor Deposition Growth and Characterization of Two-Dimensional Hexagonal Boron Nitride*. Singapore: Springer Singapore; 2018. DOI: 10.1007/978-981-10-8809-4
- [52] Chen L et al. Screw-dislocation-driven growth of two-dimensional few-layer and pyramid-like WSe₂ by sulfur-assisted chemical vapor deposition. *ACS Nano*. 2014;**8**(11):11543-11551. DOI: 10.1021/nn504775f
- [53] Zhang L et al. Three-dimensional spirals of atomic layered MoS₂. *Nano Letters*. 2014;**14**(11):6418-6423. DOI: 10.1021/nl502961e
- [54] Song X et al. Chemical vapor deposition growth of large-scale hexagonal boron nitride with controllable orientation. *Nano Research*. 2015;**8**(10):3164-3176. DOI: 10.1007/s12274-015-0816-9
- [55] Tyagi P et al. Direct growth of self-aligned single-crystalline GaN nanorod array on flexible Ta foil for photocatalytic solar water-splitting. *Journal of Alloys and Compounds*. 2019;**805**:97-103. DOI: 10.1016/j.jallcom.2019.07.071
- [56] Ramesh C et al. Effect of surface modification and laser repetition rate on growth, structural, electronic and optical properties of GaN nanorods on flexible Ti metal foil. *RSC Advances*. 2020;**10**(4):2113-2122. DOI: 10.1039/C9RA09707D
- [57] Pierret A et al. Excitonic recombinations in h - BN: From bulk to exfoliated layers. *Physical Review B*. 2014;**89**(3):035414. DOI: 10.1103/PhysRevB.89.035414
- [58] Li LH, Chen Y, Behan G, Zhang H, Petracic M, Glushenkov AM. Large-scale mechanical peeling of boron nitride nanosheets by low-energy ball milling. *Journal of Materials Chemistry*. 2011;**21**(32):11862. DOI: 10.1039/c1jm11192b
- [59] Cui Z, Oyer AJ, Glover AJ, Schniepp HC, Adamson DH. Large scale thermal exfoliation and functionalization of boron nitride. *Small*. 2014;**10**(12):2352-2355. DOI: 10.1002/smll.201303236
- [60] Yu B et al. Thermal exfoliation of hexagonal boron nitride for effective enhancements on thermal stability, flame retardancy and smoke suppression of epoxy resin nanocomposites via sol-gel process. *Journal of Materials Chemistry A*. 2016;**4**(19):7330-7340. DOI: 10.1039/C6TA01565D
- [61] Rand MJ, Roberts JF. Preparation and properties of thin film boron

nitride. *Journal of the Electrochemical Society*. 1968;**115**(4):423.
DOI: 10.1149/1.2411238

[62] Müller F, Hüfner S, Sachdev H, Laskowski R, Blaha P, Schwarz K. Epitaxial growth of hexagonal boron nitride on Ag(111). *Physical Review B*. 2010;**82**(11):113406.
DOI: 10.1103/PhysRevB.82.113406

[63] Lu G et al. Synthesis of large single-crystal hexagonal boron nitride grains on Cu–Ni alloy. *Nature Communications*. 2015;**6**(1):6160. DOI: 10.1038/ncomms7160

[64] Pakdel A, Zhi C, Bando Y, Golberg D. Low-dimensional boron nitride nanomaterials. *Materials Today*. 2012;**15**(6):256-265. DOI: 10.1016/S1369-7021(12)70116-5

[65] Lin Y, Connell JW. Advances in 2D boron nitride nanostructures: Nanosheets, nanoribbons, nanomeshes, and hybrids with graphene. *Nanoscale*. 2012;**4**(22):6908. DOI: 10.1039/c2nr32201c

[66] Gautam C, Chelliah S. Methods of hexagonal boron nitride exfoliation and its functionalization: Covalent and non-covalent approaches. *RSC Advances*. 2021;**11**(50):31284-31327. DOI: 10.1039/D1RA05727H

[67] Bresnehan MS et al. Integration of hexagonal boron nitride with quasi-freestanding epitaxial graphene: Toward wafer-scale, high-performance devices. *ACS Nano*. 2012;**6**(6):5234-5241.
DOI: 10.1021/nn300996t

[68] Tay RY et al. Trimethylamine borane: A new single-source precursor for monolayer h-BN single crystals and h-BCN thin films. *Chemistry of Materials*. 2016;**28**(7):2180-2190.
DOI: 10.1021/acs.chemmater.6b00114

[69] Müller F, Hüfner S, Sachdev H, Gsell S, Schreck M. Epitaxial growth of hexagonal boron nitride monolayers by a three-step boration-oxidation-nitration process. *Physical Review B*. 2010;**82**(7):075405.
DOI: 10.1103/PhysRevB.82.075405

[70] Wang M et al. Correction to catalytic transparency of hexagonal boron nitride on copper for chemical vapor deposition growth of large-area and high-quality graphene. *ACS Nano*. 2014;**8**(8):8711-8711. DOI: 10.1021/nn503982j

[71] Caneva S et al. Nucleation control for large, single crystalline domains of monolayer hexagonal boron nitride via Si-doped Fe catalysts. *Nano Letters*. 2015;**15**(3):1867-1875. DOI: 10.1021/nl5046632

[72] Ismach A et al. Toward the controlled synthesis of hexagonal boron nitride films. *ACS Nano*. 2012;**6**(7):6378-6385.
DOI: 10.1021/nn301940k

[73] Bansal A, Zhang X, Redwing JM. Gas source chemical vapor deposition of hexagonal boron nitride on C-plane sapphire using B₂H₆ and NH₃. *Journal of Materials Research*. 2021;**36**(23):4678-4687. DOI: 10.1557/s43578-021-00446-5

[74] Zhang C, Hao X, Wu Y, Du M. Synthesis of vertically aligned boron nitride nanosheets using CVD method. *Materials Research Bulletin*. 2012;**47**(9):2277-2281. DOI: 10.1016/j.materresbull.2012.05.042

[75] Oh H, Yi G-C. Synthesis of atomically thin h-BN layers using BCl₃ and NH₃ by sequential-pulsed chemical vapor deposition on Cu foil. *Nanomaterials*. 2021;**12**(1):80. DOI: 10.3390/nano12010080

[76] Pierson HO, Pierson HO. *Handbook of Chemical Vapor Deposition*. 2nd ed. Norwich, NY: Noyes Publications; 1999

[77] Jones AC, Hitchman ML. Chemical Vapour Deposition: Precursors, Processes and Applications. Cambridge: Royal Society of Chemistry; 2008. DOI: 10.1039/9781847558794

ACS Applied Electronic Materials. 2021;3(8):3547-3554. DOI: 10.1021/acsaelm.1c00469

[78] Farhad SFU. The effect of substrate temperature and oxygen partial pressure on the properties of nanocrystalline copper oxide thin films grown by pulsed laser deposition. Data in Brief. 2021;34:106644. DOI: 10.1016/j.dib.2020.106644

[79] Wang G et al. Direct growth of hexagonal boron nitride films on dielectric sapphire substrates by pulsed laser deposition for optoelectronic applications. Fundamental Research. 2021;1(6):677-683. DOI: 10.1016/j.fmre.2021.09.014

[80] Velázquez D, Seibert R, Man H, Spentzouris L, Terry J. Pulsed laser deposition of single layer, hexagonal boron nitride (white graphene, h-BN) on fiber-oriented Ag(111)/SrTiO₃ (001). Journal of Applied Physics. 2016;119(9):095306. DOI: 10.1063/1.4943174

[81] Jang SK, Youn J, Song YJ, Lee S. Synthesis and characterization of hexagonal boron nitride as a gate dielectric. Scientific Reports. 2016;6(1):30449. DOI: 10.1038/srep30449

[82] Dean CR et al. Boron nitride substrates for high-quality graphene electronics. Nature Nanotechnology. 2010;5(10):722-726. DOI: 10.1038/nnano.2010.172

[83] Britnell L et al. Field-effect tunneling transistor based on vertical graphene Heterostructures. Science. 2012;335(6071):947-950. DOI: 10.1126/science.1218461

[84] Ranjan A et al. Dielectric breakdown in single-crystal hexagonal boron nitride.